Biochimica et Biophysica Acta 1843 (2014) 2027–2036

Contents lists available at ScienceDirect

Biochimica et Biophysica Acta

journal homepage: www.elsevier.com/locate/bbamcr

Transport of c-MYC by Kinesin-1 for proteasomal degradation in the cytoplasm

Clement M. Lee *

Icahn School of Medicine at Mount Sinai, Department of Oncological Sciences, One Gustave L. Levy Place, Box 1130, New York, NY 10029, USA

ARTICLE INFO

Article history:
Received 14 March 2014
Received in revised form 30 April 2014
Accepted 2 May 2014
Available online 10 May 2014

Keywords:
c-MYC
Kinesin-1
Trafficking
Proteasomal degradation

ABSTRACT

c-MYC is an oncogenic transcription factor that is degraded by the proteasome pathway. However, the mechanism that regulates delivery of c-MYC to the proteasome for degradation is not well characterized. Here, the results show that the motor protein complex Kinesin-1 transports c-MYC to the cytoplasm for proteasomal degradation. Inhibition of Kinesin-1 function enhanced ubiquitination of c-MYC and induced aggregation of c-MYC in the cytoplasm. Transport studies showed that the c-MYC aggregates moved from the nucleus to the cytoplasm and KIF5B is responsible for the transport in the cytoplasm. Furthermore, inhibition of the proteasomal degradation process also resulted in an accumulation of c-MYC aggregates in the cytoplasm. Moreover, Kinesin-1 was shown to interact with c-MYC and the proteasome subunit S6a. Inhibition of Kinesin-1 function also reduced c-MYC-dependent transformation activities. Taken together, the results strongly suggest that Kinesin-1 transports c-MYC for proteasomal degradation in the cytoplasm and the proper degradation of c-MYC mediated by Kinesin-1 transport is important for transformation activities of c-MYC. In addition, the results indicate that Kinesin-1 transport mechanism is important for degradation of a number of other proteins as well.

1. Introduction

c-MYC is a major regulator of diverse physiological processes, such as proliferation, apoptosis, differentiation and genomic stability. In addition, c-MYC causes cancer when it is overexpressed [1–3]. Hence, the cellular levels of c-MYC are tightly regulated by multiple mechanisms, including degradation by the ubiquitin–proteasome pathway [4–6]. In this pathway, c-MYC is conjugated with polyubiquitin chains. The ubiquitination of c-MYC serves as a signal for c-MYC degradation by the proteasomal protein destruction machine.

Kinesins belong to a large family of intracellular molecular motors [7,8]. These molecular motors hydrolyze ATP and convert the chemical energy to mechanical energy to move along microtubules and carry their cargo, such as mRNA, membranous vesicles, organelles and protein complexes, to their specific target places [7,9,10]. Defects in these molecular motors give rise to various diseases, such as cancer, neurodegeneration and developmental defects [9,10]. Kinesin-1 is the founding member of this superfamily and is a heterotetrameric protein containing two subunits of Kinesin Light Chain 1 (KLC1) and two subunits of Kinesin Heavy Chain (KHC). KHC contains a motor domain to hydrolyze ATP and move along microtubules, while KLC1 interacts with cargoes [7]. There are three members of KHCs, namely KIF5A, KIF5B and KIF5C [7]. While KIF5B is ubiquitously expressed, KIF5A and KIF5C are neuronal specific [7].

It remains unclear how c-MYC is delivered to proteasomes for degradation. Here, the results show that c-MYC is a cargo of Kinesin-1 and that Kinesin-1 is actively involved in transporting c-MYC for proteasomal degradation in the cytoplasm.

2. Materials and methods

2.1. Materials

The following reagents were obtained commercially: anti-c-MYC antibodies [sc764 and sc-70467 (Santa Cruz); 5605 (Cell Signaling)]; anti-HA antibody [sc-7392 and sc-805 (Santa Cruz)]; anti-V5 antibody [sc-271944 and sc-83849-R (Santa Cruz)]; anti-GFP antibody [sc-9996 (Santa Cruz)]; anti-ubiquitin antibody [sc-8017 (Santa Cruz); 3933 (Cell Signaling)]; anti-p53 antibody [sc-126 (Santa Cruz)]; anti-NF-κB p65 antibody [sc-8008 (Santa Cruz)]; anti-p38MAPK antibody [8690 (Cell Signaling)]; anti-c-Fos antibody [2250 (Cell Signaling)]; anti-Rab8 antibody [6975 (Cell Signaling)]; anti-β-Actin antibody [A2228 (Sigma)]; anti-α-Tubulin [T9026 (Sigma)]; anti-KIF5B antibody [21632-1-AP (Proteintech)]; anti-KLC1 antibody [sc-13362 (Santa Cruz)]; anti-S6a antibody [PW8770 (Enzo)]; anti-S6b antibody [PW8175 (Enzo)]; anti-Skp2 [sc-7164 (Santa Cruz)]; antibody anti-CHIP antibody [PC711 (Calbiochem)]; MG132 (Boston Biochem); pTagCFP-C (Evrogen); ptdTomato and pAcGFP (Clontech).

Abbreviations: RBL, rose bengal lactone; EHNA, erythro-9-[3-(2-hydroxynonyl)] adenine; LMB, leptomycin B; KLC1, Kinesin Light Chain 1; DMSO, dimethyl sulfoxide; HMWS, high molecular-weight species; DAPI, 4′,6-diamidino-2-phenylindole

* Tel.: +1 212 659 5560.
E-mail address: clement.lee@mssm.edu.

http://dx.doi.org/10.1016/j.bbamcr.2014.05.001
0167-4889/

2.2. Cell culture

HEK293T, COS7 and HeLa were grown in Dulbecco's Modified Eagle's medium (Corning Cellgro) supplemented with 10% fetal bovine serum (Sigma, MO). Cell cultures were maintained at 37 °C with 5% CO_2.

2.3. siRNA and shRNA

HeLa cells were treated with double-stranded RNA oligonucleotide that targets the mRNA of human KIF5B (accession number: NM_004521) as described [11]: sense, 5′-UGA AUU GCU UAG UGA UGA AdTdT-3′. The control double-stranded RNA oligonucleotide against firefly luciferase has the following sequences: sense, 5′-AUGAACGUGA AUUGCUCAAdTdT-3′. All siRNAs were synthesized by Thermo Scientific. Lipofectamine 2000 (Invitrogen) was used to transfect cells. HeLa cells were subjected to at least two rounds of plating/transfection with the siRNAs to knockdown the KIF5B expression levels.

A retroviral vector expressing the shRNA against KIF5B was prepared by annealing two oligonucleotides with the sense sequence (5′-CCGG TGAATTGCTTAGTGATGAACTCGAGTTCATCACTAAGCAATTCATTTTTA ATT-3′). The annealed oligonucleotide was cloned into the AgeI and EcoRI sites of the lentiviral vector pLKO-Tet-On containing the H1 RNA promoter and a tetracycline-inducible operator [12]. A DNA fragment containing the H1 RNA promoter, the tetracycline-inducible operator and the oligonucleotide sequence was amplified from the vector, blunt-ended and cloned into MSCVhph (Clontech).

2.4. Transient transfection

For plasmid transfection, cells were transfected using Lipofectamine 2000 (Invitrogen) or XtremeGene 9 (Roche) according to the manufacturers' instructions. The plasmid/transfection reagent complex was formed in OptiMEM I (Invitrogen) and then added to cells. The transfected cells were harvested for analysis one day later.

2.5. Western blot analysis

The cell lysates or immunoprecipitates were resolved by SDS-PAGE. The resolved proteins were transferred onto nitrocellulose membranes, which were blocked in Blocking Buffer for Fluorescent Western Blotting (Rockland). Appropriate primary antibodies were added to the membranes in the blocking buffer containing 0.1% Tween-20 at 4 °C overnight. Membranes were washed three times with washing buffer (PBS/0.1% Tween-20) before they were incubated with IRDye 680RD- and IRDye800CW-conjugated secondary antibodies (Odyssey) at room temperature for an hour. The membranes were washed three times with the washing buffer and the immunoreactive protein bands were detected by the Odyssey Infrared imaging system.

2.6. Immunoprecipitation

For association studies, transfected cells were lysed in NP40 lysis buffer (0.5% NP40 in PBS) supplemented with 1 mM DTT, 6 mM NaF and protease inhibitors. For immunoprecipitation of ubiquitinated proteins, transfected cells were lysed in RIPA buffer [13] supplemented with 6 mM NaF and protease inhibitors. Appropriate antibodies were added to the cell lysates and incubated at 4 °C for 2 h before Protein G beads (GE Healthcare) were added for another hour. The beads were washed three times with the lysis buffer, resuspended in Laemmli buffer and subjected to SDS-PAGE. RIPA lysis buffer was also used for the pull-down assays of 6His-tagged proteins using nickel-agarose beads.

2.7. Immunofluorescence

These studies were conducted similarly as described [14] using specific antibodies as indicated. The nuclei of live and fixed cells were stained with Hoechst 33342 (Hoechst) and 4′,6-diamidino-2-phenylindole (DAPI), respectively. The cells were analyzed under a fluorescence microscope (Olympus IX71_Fluoview). Images were captured using DP72 Olympus camera system and cellSens software. Magnification is at 40× unless indicated otherwise.

2.8. Soft agar assay

The REF/MYC-Ras cells or cancer cells were plated in soft agar (0.3%) in the presence of DMSO or rose bengal lactone (RBL; 40 μM). They were maintained at 37 °C with 5% CO_2. Fresh medium was added every four to five days. Photographs were taken for the colonies 4 and 17 days after plating, respectively. The infected REF/MYC-Ras cells were also similarly plated in soft agar.

3. Results

3.1. The effects of the Kinesin-1 inhibitor RBL on c-MYC

To study the effects of Kinesin-1 on c-MYC, three different strategies to inhibit Kinesin-1 were employed: 1) the KIF5B inhibitor rose bengal lactone (RBL), which inhibits the interaction between Kinesin-1 and microtubules [15], 2) small interfering RNA (siRNA) against KIF5B and 3) a truncated mutant of KIF5B that inhibits the wild-type KIF5B functions. Treatment of cells with the Kinesin-1 inhibitor (RBL) [15] showed decreased levels of endogenous c-Myc (64 kDa) with a corresponding increase in high-molecular weight species (HMWS) in both HEK293T and HeLa cells (Fig. 1A). Interestingly, RBL also induced HMWS formation of α-Tubulin with an intense 140 kDa protein band (Supplementary Fig. 1). However, RBL did not induce HMWS formation of β-Actin (Fig. 1A and Supplementary Fig. 1). The HMWS could be detected by various specific antibodies against different epitopes of c-MYC (Fig. 1A and Supplementary Fig. 1) and the effects of RBL were dose-dependent (Supplementary Fig. 2). Furthermore, formation of HMWS could only be observed following treatment with the Kinesin-1 inhibitor RBL, but not following treatment with the inhibitor of another motor protein Dynein [erythro-9-[3-(2-hydroxynonyl)] adenine (EHNA)] [16] (Supplementary Fig. 3). Because the motor proteins Kinesin-1 and Dynein are responsible for anterograde and retrograde movements, respectively [11,17–19], these results suggest that anterograde, but not retrograde, movement by Kinesin-1 was involved in the formation of the HMWS of c-MYC.

To determine whether the observed HMWS is, in fact, a ubiquitinated form of c-MYC, HEK293T cells were transfected with 6His-tagged ubiquitin [20] and subsequently treated with vehicle (DMSO) or RBL. After RBL treatment, 6His-tagged ubiquitinated proteins were pulled down using nickel-agarose beads and the resulting precipitates were analyzed using a c-MYC specific antibody to detect ubiquitinated c-MYC. The results in Fig. 1B show that ubiquitination of c-MYC was enhanced by treatment with RBL, indicating that Kinesin-1 is involved in the proteasomal degradation of c-MYC. Similar results were obtained with exogenous HA-tagged c-MYC (Fig. 1C) and endogenous c-MYC (Fig. 1D). c-MYC is ubiquitinated by several E3 ubiquitin ligases, such as Skp2, CHIP, Fbw7 and Pirh2 [21–24]. Attempts were made to identify the E3 ubiquitin ligases involved in the RBL-mediated ubiquitination of c-MYC. Results in Supplementary Fig. 4A and B show that ablation of Skp2 and CHIP enhanced the endogenous c-MYC levels especially in HEK293T cells. However, ubiquitinated (HMWS) c-MYC was not reduced, suggesting that the E3 ubiquitin ligases Skp2 and CHIP are not involved in the RBL-mediated ubiquitination of c-MYC. To determine the subcellular localization of ubiquitinated c-MYC, HeLa cells were treated with DMSO or RBL and then fractionated into the cytoplasmic and nuclear fractions. While the results do not rule out the possibility of ubiquitination of c-MYC induced by RBL in the cytoplasm (Supplementary Fig. 5), they do show that ubiquitinated (HMWS) c-MYC was found in both cytoplasmic and nuclear fractions,

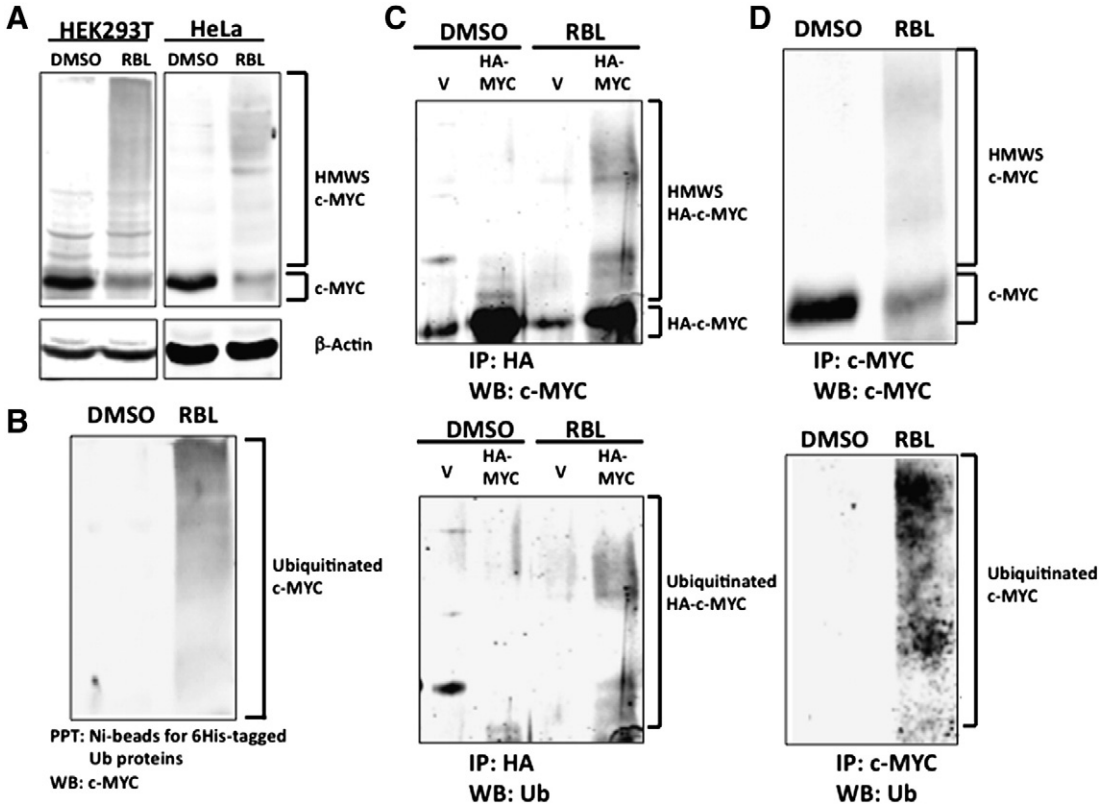

Fig. 1. Kinesin-1 inhibitor RBL increases ubiquitinated c-MYC levels. A: HEK293T and HeLa cells were treated with DMSO or rose bengal lactone (RBL; 40 μM) for 16 h. Cell lysates were prepared and endogenous levels of c-MYC and β-Actin were analyzed by western blot analysis using specific antibodies against c-MYC [5605 (Cell Signaling)] and β-Actin. The high molecular-weight species (HMWS) of c-MYC is shown in the RBL-treated cells. B: HEK293T cells were transfected with 6His-tagged Ubiquitin (Ub) and then treated with DMSO or RBL. The cell lysates from the treated cells were mixed with nickel-agarose beads to pull down 6His-tagged (ubiquitinated) proteins. The precipitates were analyzed by western blotting using the specific antibodies against c-MYC. C: HEK293T cells were transfected with an empty vector (V) or a vector expressing the exogenous HA-tagged c-MYC. After transfection, the cells were treated with DMSO or RBL (40 μM) for 16 h. Cell lysates were prepared and immunoprecipitated with the HA tag specific antibody. The lysates together with the immunoprecipitates were analyzed by western blot using specific antibodies against c-MYC (upper panel) and Ub (lower panel). The high molecular-weight species (HMWS) of c-MYC is indicated. D: Cells were treated as described in C, except that endogenous c-MYC was immunoprecipitated with its specific antibody [sc-40 (Santa Cruz)]. All the experiments were repeated at least twice.

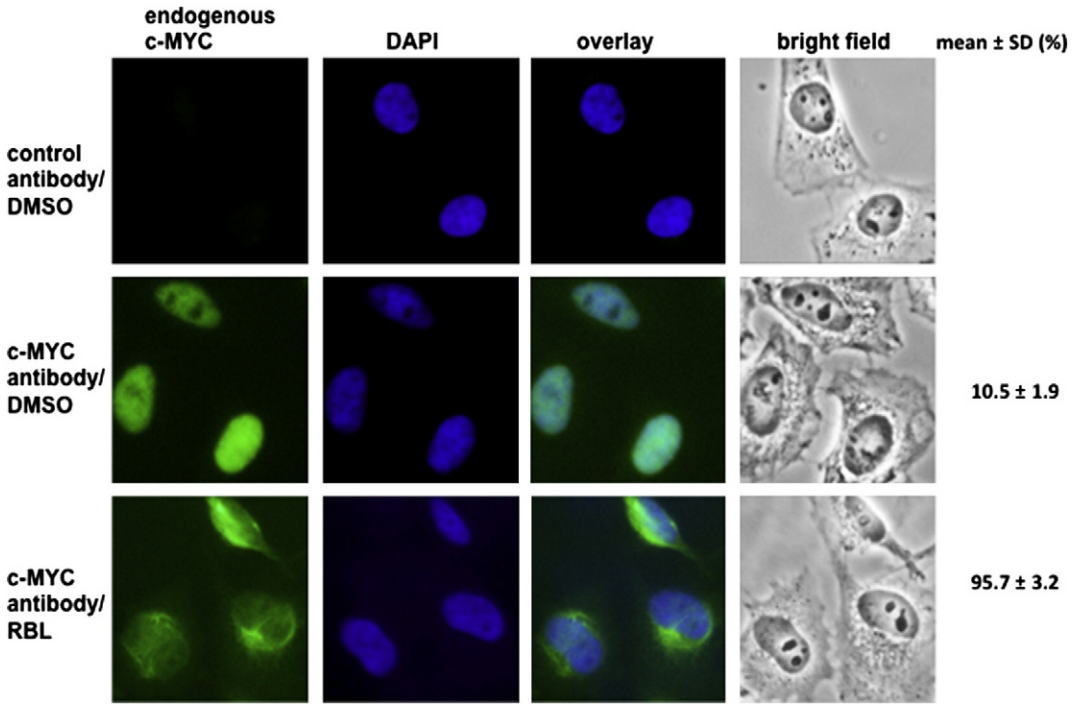

Fig. 2. RBL induces aggregation of c-MYC. HeLa cells were treated with DMSO or RBL for 18 h and then fixed and probed with a control antibody or c-MYC antibody together with DAPI. The cells were then examined under a fluorescent microscope. The percentages of cells showing c-MYC aggregates in the cytoplasm were scored and the results are presented as mean ± SD (N = 3). Total number of cells examined was greater than 900. Morphology of the cells is also shown (bright field).

indicating that RBL-mediated ubiquitination of c-MYC occurred in the nucleus and that ubiquitinated c-MYC was transported into the cytoplasm.

To determine the effects of RBL on endogenous c-MYC at the cellular level, immunofluorescence studies were performed in HeLa cells, which were treated with vehicle (DMSO) or RBL. Results in Fig. 2 show that the endogenous c-MYC mainly appeared in the nucleus in DMSO-treated cells; however, upon the RBL treatment, c-MYC aggregated in the cytoplasm, suggesting that Kinesin-1 regulates the subcellular localization of c-MYC.

To determine whether the formation of HMWS is a general property associated with RBL treatment, a panel of cytoplasmic and nuclear proteins were analyzed in cells that have been treated with DMSO or RBL. Results in Fig. 3 show that among the proteins examined, c-MYC, p53, KIF5B and α-Tubulin were most affected by RBL, suggesting that Kinesin-1 is also involved in their proteasomal degradation. However, RBL treatment induced low levels of p38MAPK, NF-κB p65 and c-Fos HMWS and β-Actin did not form any HMWS, indicating that proteasomal degradation of these proteins is not regulated by Kinesin-1.

3.2. The effects of the dominant negative mutant of KIF5B on c-MYC

To confirm that the above observation was due to the specific inhibition of KIF5B by RBL, two additional strategies were employed to inhibit KIF5B: overexpression of a KIF5B dominant negative mutant and a siRNA against KIF5B. First, c-MYC was co-expressed with wild-type KIF5B or a motorless KIF5B mutant that lacks the motor domain but retains the ability to dimerize with wild-type KIF5B. To assess the role of Kinesin-1 in regulating the subcellular localization of c-MYC, TagCFP-c-MYC was co-expressed in HeLa cells with wild-type or motorless tdTomato-tagged KIF5B mutant and live-cell fluorescence microscopy was performed to determine subcellular localization. The results in Fig. 4A show that in HeLa cells, c-MYC and wild-type KIF5B mainly localized in the nucleus and cytoplasm, respectively. However, the motorless KIF5B mutant appeared as punctate or filamentous aggregates as described previously [19]. Expression of the motorless KIF5B mutant resulted in the appearance of a fraction of c-MYC in the cytoplasm, whereby both proteins co-localized together, suggesting that KIF5B regulates the subcellular localization of c-MYC (Fig. 4A). A similar phenotype was also observed in H1299 cells, suggesting that the regulation of c-MYC subcellular localization induced by KIF5B is not unique to HeLa cells (Supplementary Fig. 6). Aggregation of endogenous c-MYC was also induced by the motorless KIF5B mutant, but not by the wild-type KIF5B (Fig. 4B). On the other hand, expression of the motorless KIF5B mutant did not induce any appearance of AcGFP-c-Fos in the cytoplasm (Supplementary Fig. 7), indicating that inhibition of KIF5B function specifically affects certain transcription factors. In addition, expression of the neuronal motorless KIF5A mutant also formed aggregates in the cytoplasm, but failed to induce the aggregates of c-MYC in the cytoplasm (Supplementary Fig. 8). This further shows that KIF5B is the specific motor transporter of c-MYC in these cells. In addition, the motorless KIF5B mutant induced aggregation of part of the α-Tubulin network, but not that of β-Actin, suggesting that KIF5B preferentially disrupts part of the cytoskeletal organization of α-Tubulin (Supplementary Fig. 9). Moreover, the motorless KIF5B mutant did not induce any change in the subcellular localization of the Rab8 GTPase, suggesting that KIF5B is not involved in the vascular traffic between the trans-Golgi network and basolateral membrane of the Rab8 GTPase (Supplementary Fig. 10) [25]. Together, the data suggest that KIF5B is a specific regulator of c-Myc transport.

3.3. The direction of transport of c-MYC mediated by KIF5B

To determine the direction of c-MYC transport, cells expressing TagCFP-c-MYC and tdTomato-wild-type and motorless KIF5B mutant were treated with the nuclear export inhibitor leptomycin B (LMB) [26]. The results in Fig. 4C show that LMB treatment prevented c-MYC, but not the motorless KIF5B mutant, from forming aggregates in the cytoplasm. In contrast, in the DMSO control, both c-MYC and motorless KIF5B formed aggregates in the cytoplasm. This result shows that c-MYC is transported from the nucleus to the cytoplasm and that the c-MYC aggregates are not derived from the newly synthesized pool of c-MYC in the cytoplasm. Because KIF5B is an anterograde motor, moving on microtubule originating from the microtubule organizing center in the perinuclear region to the cell periphery [27,28], this result suggests that KIF5B is responsible for the transport of c-MYC in the cytoplasm during the process.

3.4. Co-localization of c-MYC and KIF5B in the cytoplasm

To show the association between c-MYC and KIF5B in the cell, immunofluorescence studies were performed in HeLa cells expressing HA-tagged c-MYC and tdTomato-tagged KIF5B. The results in Fig. 5 show that, upon high magnification (100×), tdTomato-tagged KIF5B mainly appeared in a punctate distribution in the cytoplasm and majority of HA-tagged c-MYC appeared in the nucleus. A longer exposure shows that HA-c-MYC could be detected as fine spots in the cytoplasm. Some co-localized with tdTomato-KIF5B in the cytoplasm, suggesting that c-MYC and KIF5B move together as a complex in the cytoplasm for degradation. It is worth noting that some c-MYC punctations did not co-localize with tdTomato-KIF5B and this may represent newly synthesized c-MYC in the cytoplasm. To further show that KIF5B is involved

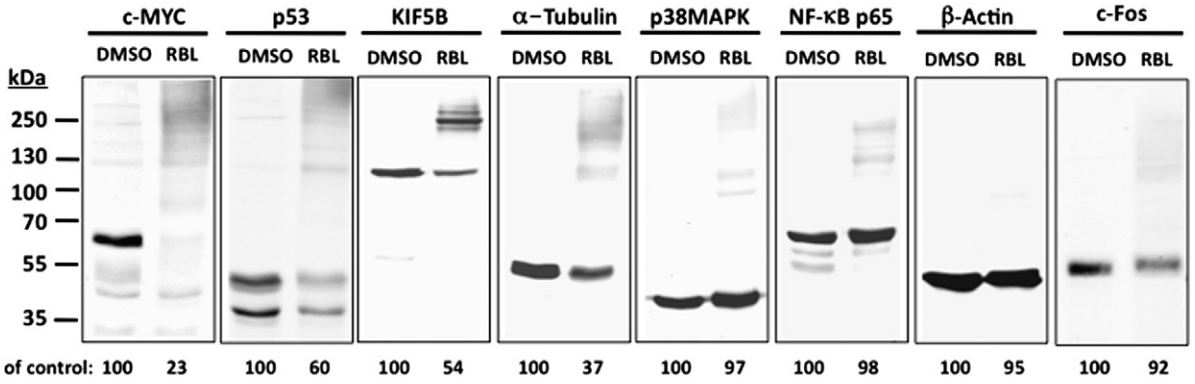

Fig. 3. RBL increases the formation of HMWS of cytoplasmic and nuclear proteins. HEK293T cells were treated with DMSO or RBL (40 μM) for 16 h. The cell lysates from the treated cells were analyzed by western blotting with specific antibodies against c-MYC, p53, NF-κB p65, KIF5B, p38MAPK, α-Tubulin and β-Actin. The molecular weight markers in kDa are indicated. The signals of the unmodified specific proteins in the DMSO- or RBL-treated samples were quantitated and their relative levels are quoted. For c-Fos, exogenous protein was expressed in the cells before they were treated with DMSO or RBL. All the experiments were repeated at least twice.

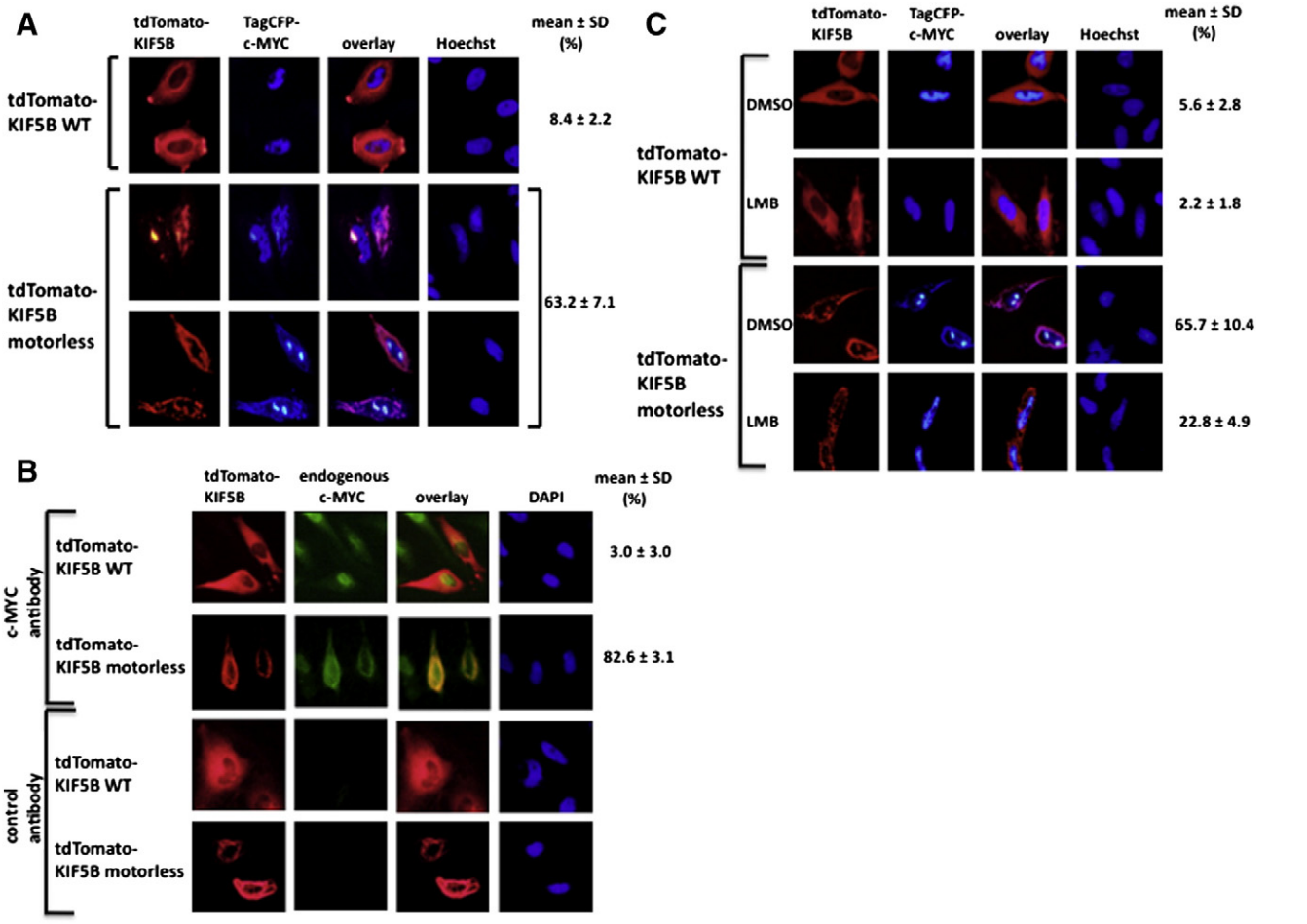

Fig. 4. Expression of the motorless KIF5B mutant induces c-MYC appearance in the cytoplasm. A: HeLa cells were transfected with tdTomato-tagged wild-type (WT) or motorless KIF5B mutant together with TagCFP-c-MYC. 18 h after transfection, they were stained with the DNA intercalating dye Hoechst and then examined under a fluorescence microscope. The percentages of cells showing aggregates of CFP-c-MYC are shown. The results are presented as mean ± SD (N = 3). Total number of cells examined was greater than 370. B: Cells were transfected with the WT or motorless tdTomato-KIF5B mutant. 18 h later, the cells were fixed and probed for the endogenous c-MYC using its specific antibody and the DNA intercalating dye DAPI. They were then examined under a fluorescence microscope. The percentages of transfected cells showing c-MYC aggregates were scored and the results are presented as mean ± SD (N = 3). Total number of cells examined was greater than 400. C: Cells were transfected with the WT or motorless tdTomato-KIF5B mutant together with TagCFP-c-MYC. 8 h after transfection, cells were treated with vehicle (DMSO) or the nuclear export inhibitor leptomycin B (LMB) (100 ng/ml). 16 h after the LMB treatment, the cells were stained with the DNA intercalating dye Hoechst and then examined under a fluorescence microscope. Proteins tagged with tdTomato and TagCFP appear red and blue, respectively. Co-localization of proteins with both tags appears pink. The percentages of cells showing aggregates of CFP-c-MYC are shown. The results are presented as mean ± SD (N = 3). Total number of cells examined was greater than 1500.

in forming a protein complex with c-MYC for its degradation, a set of cells was deprived of serum for 60 min before analysis since serum deprivation is known to induce degradation of c-MYC [29]. Results in Fig. 5 show that a higher amount of c-MYC appeared in the cytoplasm when the cells were deprived of serum, suggesting that degradation of c-MYC happens in the cytoplasm. Moreover, a high percentage of c-MYC in the cytoplasm under this condition co-localized with KIF5B, suggesting that these proteins form complexes and the complex formation is involved in c-MYC degradation.

3.5. The effects of the siRNA against KIF5B on c-MYC

To further confirm the specific inhibition of KIF5B by RBL, the expression of KIF5B was knocked-down using a KIF5B-specific siRNA (siKIF5B) (Fig. 6A) [30]. The results in Fig. 6B show that ablation of KIF5B expression by siKIF5B induced accumulation of c-MYC aggregates in the cytoplasm, while no c-MYC aggregated in the cytoplasm when the cells were treated with the control siRNA, indicating that KIF5B is important in transporting c-MYC in the cytoplasm.

3.6. Aggregation of c-MYC and KIF5B in the cytoplasm induced by inhibition of proteasomal degradation of c-MYC

To confirm the involvement of Kinesin-1 in transporting c-MYC for proteasomal degradation, cells expressing TagCFP-c-MYC and tdTomato-wild-type KIF5B were treated with a proteasomal inhibitor MG132 [31]. The results in Fig. 7 show that inhibition of c-MYC degradation by MG132 also induced aggregation and co-localization of the wild-type KIF5B and c-MYC in the cytoplasm. Therefore, perturbation of proteasomal degradation process results in an accumulation of c-MYC in the cytoplasm, leading to formation of cytoplasmic aggregates. Together, the data strongly indicate that c-MYC is transported to the cytoplasm by KIF5B for proteasomal degradation.

3.7. Association between c-MYC and Kinesin-1

Kinesin-1 is a heterotetramer consisting of two subunits of KIF5B and two subunits of KLC1 [7]. The N-terminal motor domain of KIF5B interacts with and moves along a microtubule, and the C-terminal

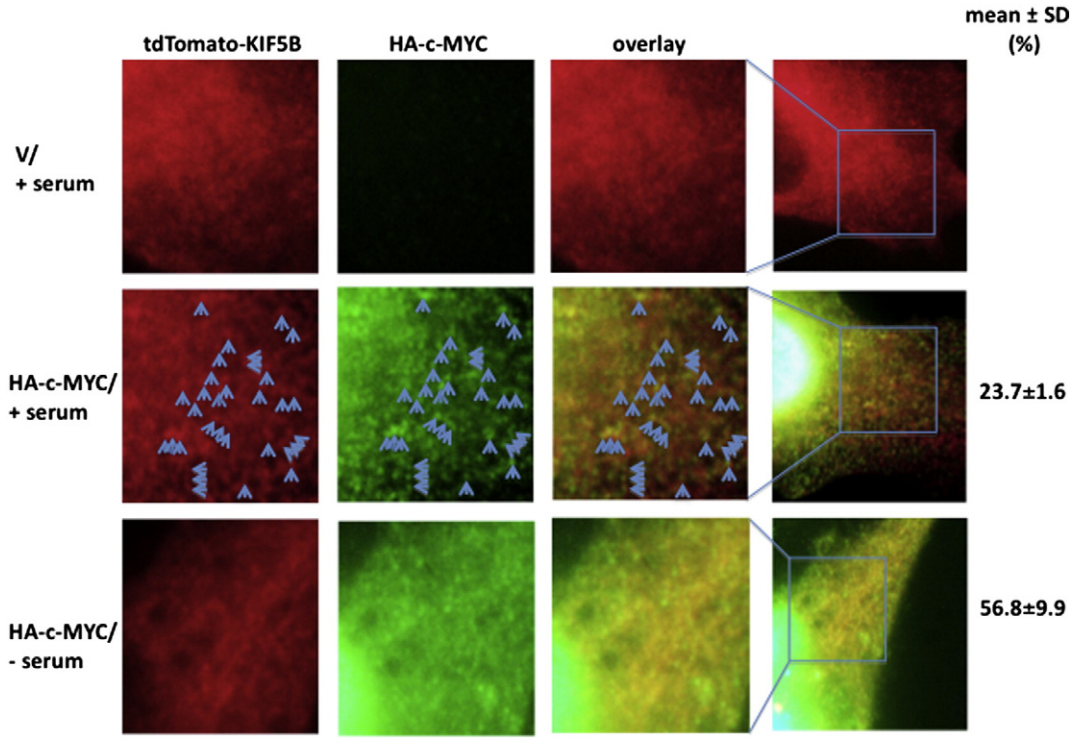

Fig. 5. Co-localization of c-MYC and KIF5B in the cytoplasm. HeLa cells were transfected with an expression vector for tdTomato-KIF5B together with an empty vector (V) or an expression vector for HA-tagged c-MYC. 18 h after transfection, a set of cells was deprived of serum (−serum) for 60 min. The cells were then fixed and stained with the specific antibody against the HA tag. The stained cells in the rightmost panel were examined under a fluorescent microscope using the 60× objective. The signals of the HA-tagged c-MYC are overexposed to show c-MYC appearance in the cytoplasm. The areas indicated by boxes in the rightmost panel were shown at the 100× magnification. Overlapping c-MYC and KIF5B are indicated by arrows in the middle panel, while the overlapping of the two proteins in the bottom panel is too numerous to be indicated. HA-c-MYC and tdTomato-KIF5B appear green and red, respectively. Co-localization of proteins with both tags appears orange. The percentages of c-MYC dots overlapping with KIF5B were scored and the results are presented as mean ± SD (N = 3).

coiled-coil domain interacts with KLC1. It is KLC1 that interacts with the scaffolding protein/cargo complexes [32]. To examine whether c-MYC interacts with Kinesin-1, immunoprecipitation studies were performed using cell lysates from transfected HEK293T cells expressing V5-tagged c-MYC with or without tdTomato-tagged KIF5B. tdTomato-tagged KIF5B was immunoprecipitated using the antibody against tdTomato. The immunoprecipitates and lysates were then analyzed by western blotting using antibodies against c-MYC and tdTomato. The results show that tdTomato-KIF5B could be co-immunoprecipitated with V5-c-MYC (Fig. 8A), indicating that c-MYC and KIF5B interact. A similar experiment was performed in cells expressing V5-tagged c-MYC with or without HA-tagged KLC1. HA-tagged KLC1 was precipitated using an antibody directed against the HA-tag. The immunoprecipitates and lysates were then analyzed by western blotting using antibodies against HA-tag and c-MYC. The results show that V5-c-MYC could be co-immunoprecipitated with HA-KLC1 (Fig. 8B), suggesting that c-MYC and KLC1 interact with each other. Together, the results suggest that c-MYC interacts with the Kinesin-1 complex (KIF5B/KLC1). The domain of KLC1 that interacts with c-MYC was mapped by immunoprecipitation studies using the wild-type (WT) or deletion mutants (TPR1 or TPR2) of HA-tagged KLC1. The results in Fig. 8C show that deletion of the N-terminal coiled-coil domain of KLC1 abolished the association of KLC1 and c-MYC, indicating that the N-terminus of KLC1 is important in the interaction with c-MYC. To further illustrate the importance of the N-terminal region of KLC1 in binding c-MYC, immunoprecipitation studies using the HA-tagged N-terminal region of KLC1(CC) and V5-tagged c-MYC were performed. Immunoprecipitation of KLC1(CC) using the HA antibody could co-precipitate c-MYC (Fig. 8D), indicating

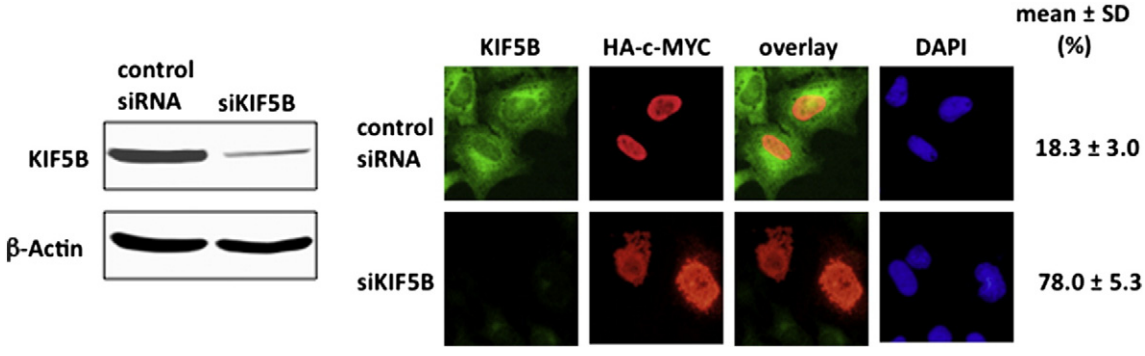

Fig. 6. Ablation of KIF5B induces aggregation of c-MYC in the cytoplasm. A: HeLa cells were transfected with a control siRNA or the siRNA against KIF5B (siKIF5B). Nine days later, the cells were lysed for western blotting using the KIF5B and β-Actin antibodies. B: The siRNA-transfected cells were also transiently transfected to express HA-tagged c-MYC. 18 h later, the cells were fixed and probed using specific antibodies against KIF5B (green), HA tag (red) and the DNA intercalating dye DAPI. They were then examined under a fluorescence microscope. The percentages of cells showing aggregates of HA-c-MYC are shown. The results are presented as mean ± SD (N = 3). Total number of cells examined was greater than 1200.

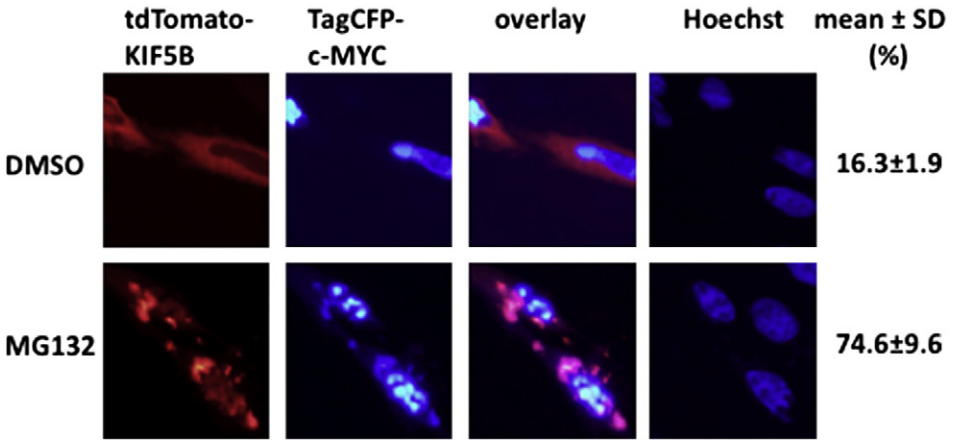

Fig. 7. Proteasomal inhibitor MG132 induces aggregation of KIF5B and c-MYC in the cytoplasm. HeLa cells were transfected to express TagCFP-tagged c-MYC together with tdTomato-tagged KIF5B. 8 h after transfection, the cells were treated with DMSO or the proteasome inhibitor MG132 (4 μM). 18 h after transfection, they were stained with the DNA intercalating dye Hoechst and then examined under a fluorescence microscope. The percentages of cells showing aggregates of CFP-c-MYC are shown. The results are presented as mean ± SD (N = 3). Total number of cells examined was greater than 600. tdTomato-KIF5B and TagCFP-c-MYC appear red and blue, respectively. Pink color indicates co-localization of proteins with both tags.

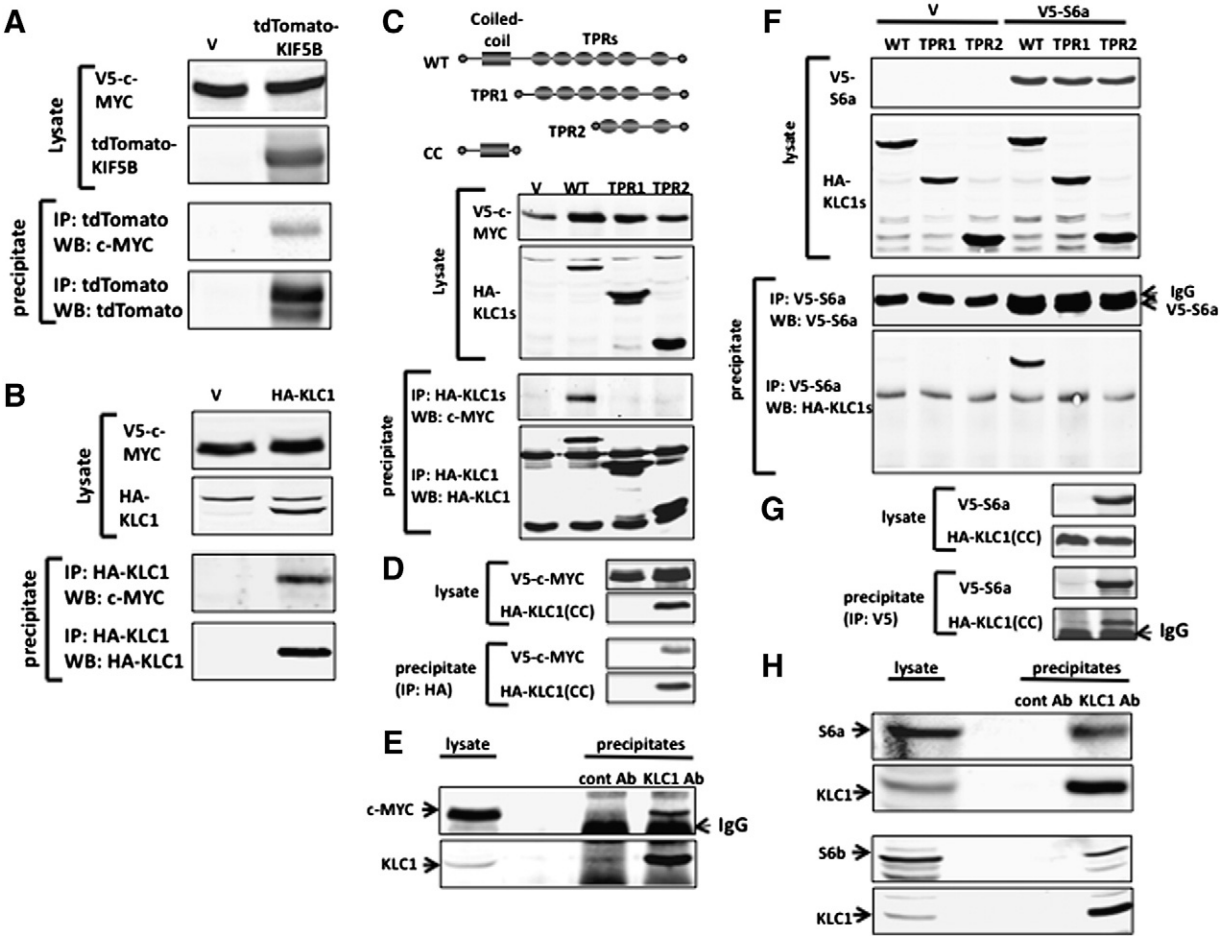

Fig. 8. Interaction of Kinesin-1 with c-MYC and the proteasome subunit S6a. A: HEK293T cells were transfected with an expression plasmid for V5-c-MYC together with an empty vector (V) or an expression vector for tdTomato-KIF5B. Cell lysates were prepared from the transfected cells for immunoprecipitation using the tdTomato antibody. The lysates and immunoprecipitates were analyzed by western blotting using the c-MYC and tdTomato antibodies. B: Cells were transfected with an empty vector (V) or HA-tagged KLC1 expression plasmid together with V5-tagged c-MYC. Cell lysates from the cells were immunoprecipitated with the antibody against HA-tag. The immunoprecipitates and lysates were analyzed by western blotting using antibodies against HA-tag and c-MYC. C: The upper panel shows a diagrammatic representation of wild-type (WT) KLC1 or its deletion mutants (CC, TPR1 and TPR2). The lower panel shows the immunoprecipitation studies as described in A using cells transfected with V5-tagged c-MYC and HA-tagged KLC1 proteins. D: The association study between the V5-tagged c-MYC and the N-terminal of KLC1 (CC; amino acids: 1–221) was performed as in C. E: Cell lysate from HEK293T cells was immunoprecipitated with a control antibody or a specific antibody against KLC1. The lysate and the immunoprecipitates were analyzed by western blotting using the antibodies against c-MYC and KLC1. F: HEK293T cells were transfected with an empty vector (V) or an expression plasmid for the V5-tagged proteasome subunit S6a together with a plasmids for the HA-tagged KLC1 proteins. Cell lysates from the transfectants were immunoprecipitated with the anti-V5 antibody. Western blot analysis was performed on the immunoprecipitates together with the cell lysates using the antibodies against V5 and HA. G: The association study between the V5-tagged S6a and KLC1(CC) was conducted as in F. The transfected cells were treated with MG132 (10 μM) for 4 h to stabilize the CC protein levels before cell lysates were prepared for the association studies. H: HEK293T cell lysate was immunoprecipitated with a control antibody or the KLC1 antibody. The lysate and immunoprecipitates were analyzed by western blotting using the antibodies against S6ba, S6b and KLC1. All the experiments were repeated at least twice.

that the N-terminal region of KLC1 containing of the coiled-coil domain is involved in binding to c-MYC. The formation of the c-MYC/KLC1 complex was substantiated by immunoprecipitation studies of the endogenous proteins. HEK293T cell lysates were immunoprecipitated with a control antibody or a specific antibody against KLC1. The KLC1 immunoprecipitate, but not the control immune-precipitate, was found to contain c-MYC (Fig. 8E). Together, the results show that c-MYC and KLC1 associate to form a complex.

3.8. Association between KLC1 and the proteasome subunit S6a

To examine whether Kinesin-1 also interacts with the proteasome, HEK293T cells were transfected with an empty vector or an expression plasmid encoding the V5-tagged proteasome subunit S6a [33] together with the wild-type, TPR1 or TPR2 of the HA-tagged KLC1. S6a is involved in interacting with incoming protein p53 for proteasomal degradation [33]. It is possible that the motor protein KLC1 that delivers c-MYC for degradation may also interact with S6a. After transfection, cell lysates were prepared and immunoprecipitated with the V5 antibody. The immunoprecipitates and the lysates were then subjected to western blot analysis. The results in Fig. 8F show that the proteasome subunit S6a associated with WT KLC1, but not with the KLC1 mutants TPR1 and TPR2, indicating that S6a interacts with the N-terminal region of KLC1 and that Kinesin-1 may be delivering its cargoes to the proteasome for degradation. To further show the importance of the N-terminal region of KLC1 in binding S6a, immunoprecipitation studies were conducted with cell lysates expressing the HA-tagged CC of KLC1 with or without V5-tagged S6a. Results in Fig. 8G show that immunoprecipitation of V5-S6a could pull down HA-CC, suggesting that the N-terminal region of KLC1 containing the coiled-coil domain is involved in binding S6a. The complex formation between KLC1 and S6a was further shown by immunoprecipitation studies using the endogenous proteins. HEK293T cell lysates were immunoprecipitated with a control antibody or a specific antibody against KLC1. The KLC1 immunoprecipitate, but not the control, was found to co-precipitate S6a (Fig. 8H), showing that KLC1 and S6b interact in vivo. In addition, another endogenous proteasomal subunit S6b was also found to associate with KLC1 using a similar association study (Fig. 8H).

3.9. The effects of Kinesin-1 inhibition on transformation activities of c-MYC

To examine the biological effects of Kinesin-1 inhibition on transformation, anchorage-independent growth of rat embryonic fibroblasts (REFs) transformed co-operatively by exogenous c-MYC and activated H-Ras (REF/MYC-Ras cells) [34] was examined. The cells were seeded in soft agar with DMSO or RBL and permitted to grow until colonies appeared. The results in Fig. 9A show that RBL inhibited the anchorage-independent growth of the cells while the DMSO-treated cells grew into colonies within four days, suggesting that Kinesin-1 function and c-MYC ubiquitination/degradation are necessary for transformation mediated by c-MYC. Focus-forming assays were also performed to further show the effects of Kinesin-1 inhibition on transformation mediated by c-MYC. The REF/MYC-Ras cells were plated in culture dishes in the presence of DMSO or RBL. The DMSO-treated cells formed foci, while the RBL-treated cells became more fibroblast-like and flat (Fig. 9B), indicating that inhibition of Kinesin-1 also reduces focus-forming ability by c-MYC. The inhibition was not due to non-specific cell death induced by RBL because when the growth rate of

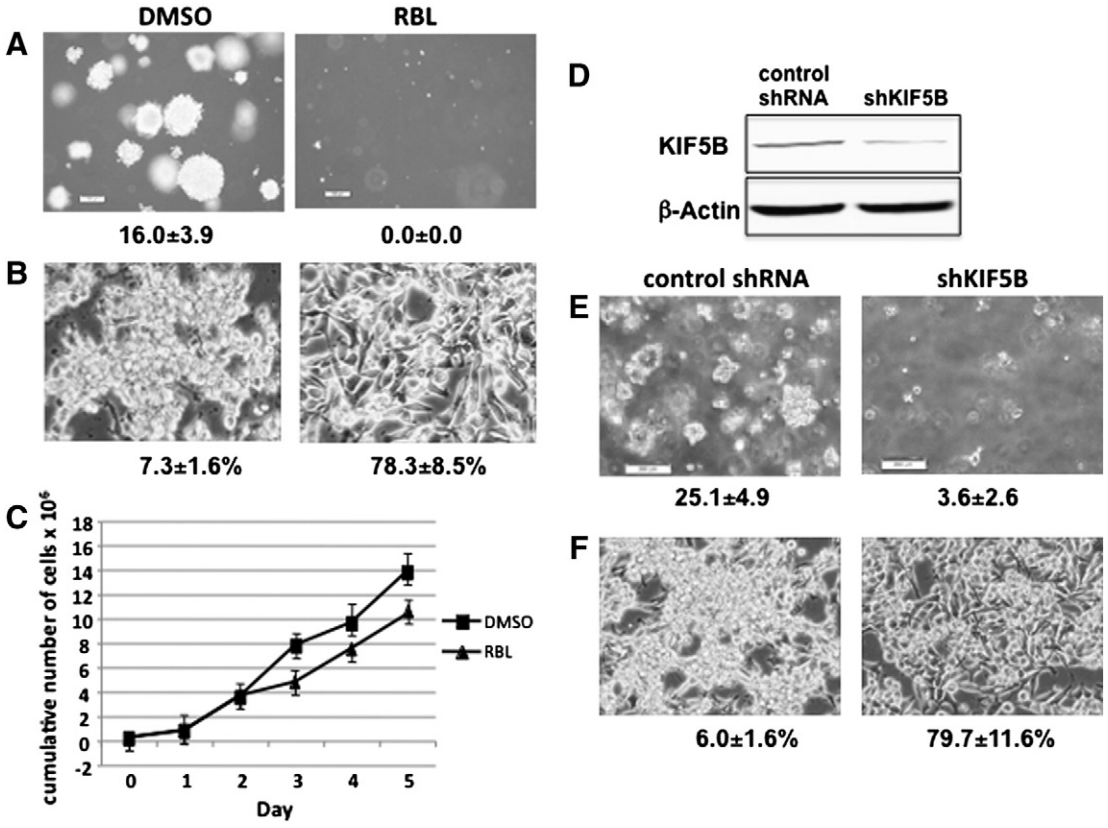

Fig. 9. Inhibition of Kinesin-1 reduces transformation activities of REF/MYC-Ras cells. A: REF/MYC-Ras cells were plated in soft agar in the presence of DMSO or RBL (40 μM). Photographs of their colonies were taken 4 days after plating. Scale bar, 100 μm. Colonies bigger than 50 μm were scored and the results are presented as mean ± SD. B: Morphology of REF/MYC-Ras cells grown in culture dishes is shown. The percentages of fibroblast-like cells were scored and the results are presented as mean ± SD. C: REF/MYC-Ras cells were seeded on day 0 in the presence of DMSO or RBL. The total number of cells was determined each day and the average number has been plotted. D: REF/MYC-Ras cells were infected with retrovirus for a control shRNA or shKIF5B. Western blotting results of the infected cells are shown. Similar experiments were performed as in B and C with the infected cells grown in soft agar (E) and in culture dishes (F). Scale bar in E, 200 μm. All the experiments were repeated at least three times.

the RBL-treated cells was determined, it was similar to the DMSO treated cells, although a noticeable reduction in their growth rate was apparent from the third day of the incubation with RBL (Fig. 9C). Furthermore, similar inhibition of transforming activities by RBL was also observed in 5 additional cancer cell lines originating from various tumor types (Supplementary Fig. 11).

To confirm reduction of transformation activities of c-MYC by inhibiting Kinesin-1, REF/MYC-Ras cells were infected to express the shRNA against KIF5B (shKIF5B) or the control shRNA. The infected cells were selected by hygromycin and then seeded for soft agar assays. Western blotting results in Fig. 9D show that shKIF5B reduced KIF5B in REF/MYC-Ras cells, compared with that in the control shRNA-treated cells. The results in Fig. 9E show that ablation of KIF5B reduced the anchorage-independent growth of the cells while the control shRNA-treated cells grew into colonies within four days, confirming that KIF5B is necessary for transformation mediated by c-MYC. Focus-forming assays were also performed to further show the effects of Kinesin-1 inhibition on transformation mediated by c-MYC. The REF/MYC-Ras cells infected with shKIF5B or the control shRNA were plated in culture dishes. The control shRNA-treated cells formed foci, while the shKIF5B-treated cells became more fibroblast-like and flat (Fig. 9F), indicating that ablation of KIF5B also reduces focus-forming ability by c-MYC. Together, the results show that KIF5B is important for transformation mediated by c-MYC.

4. Discussion

To date, this is the first report that describes the following: c-MYC is a cargo of Kinesin-1, the proteasome is one of the Kinesin-1 destinations and Kinesin-1 is important in transporting c-MYC for proteasomal degradation in the cytoplasm. When the transport of ubiquitinated c-MYC is inhibited, c-MYC forms aggregates in the cytoplasm, suggesting that the nuclear transcription factor c-MYC is actively transported by Kinesin-1 to the proteasome for degradation in the cytoplasm. This constitutes a previously undiscovered layer of post-translational regulation of c-MYC at the protein level by Kinesin-1. Furthermore, the results suggest that the transport direction is from the nucleus to the cytoplasm, which is further supported by the experiments using the nuclear export inhibitor leptomycin B (Fig. 4C). These results are consistent with the anterograde transport of Kinesin-1. In general, microtubules are arranged with their minus ends clustered around the microtubule organizing center near the nucleus and their plus ends pointing toward the cell periphery [27]. Kinesin-1 is a plus-end-directed motor that moves from the perinuclear region toward the plus ends of microtubules in the cell periphery [9,27,28,35]. Therefore Kinesin-1 is responsible for the transport of c-MYC in the cytoplasm, while another unidentified mechanism is responsible for transporting c-MYC out of the nucleus. Fig. 3 shows that other nuclear and cytoplasmic proteins formed HMWS when the cells were treated with RBL, suggesting that the transport mediated by Kinesin-1 is a more general mechanism employed by some proteins for their proteasomal degradation. It is worth noting that c-Fos shows weak formation of HMWS upon RBL treatment (Fig. 3) and it did not show any aggregation in the cytoplasm when the KIF5B motorless mutant was co-expressed (Supplementary Fig. 7), suggesting that c-Fos is not degraded in the cytoplasm via the KIF5B-dependent mechanism. It is possible that c-Fos is degraded in the nucleus or in the cytoplasm via another transport mechanism.

Proteasomes are distributed in the nucleus and in the cytoplasm, where some are associated with the endoplasmic reticulum membrane [36,37]. Proteasomal degradation occurs in those subcellular compartments. It is intriguing to find that the nuclear factor c-MYC is degraded in the cytoplasm although the c-MYC ubiquitin ligases (Fbw7 isoforms) are found in the nucleus [24]. In the current study, more c-MYC/KIF5B complexes were formed in the cytoplasm when c-MYC was induced for degradation by serum deprivation (Fig. 5), indicating that the cytoplasm is an important site for c-MYC degradation. Furthermore, it is shown that ubiquitinated c-MYC induced by RBL is found in both the nucleus and cytoplasm (Supplementary Fig. 5). It suggests that c-MYC is ubiquitinated in the nucleus and then exported to the cytoplasm for degradation or degradation of c-MYC occurs in the nucleus and cytoplasm. It has been reported that the transcription factor p53, a short-lived protein, is also transported from the nucleus to the cytoplasm for proteasomal degradation [38,39]. Interestingly, p53 also forms HMWS upon RBL treatment (Fig. 3), suggesting that p53, like c-MYC, is also degraded in the cytoplasm through the KIF5B-dependent mechanism. It is also interesting to note that the other components of the transport system KIF5B and α-Tubulin also form HMWS upon RBL treatment (Fig. 3).

It is possible that c-MYC is degraded in the cytoplasm because c-MYC is not properly recognized or accessible by the nuclear or nucleolar proteasomes under certain conditions. Alternatively, it may be faster to export c-MYC out of the nucleus to reduce c-MYC function. It is worth noting that, in addition to the cytoplasmic proteasomal system, the lysosomal system also mediates protein degradation [40–42]. However, when Kinesin-1 is inhibited, c-MYC still forms aggregates in the cytoplasm that are not cleared by the lysosomal degradation system, suggesting that the anterograde motor Kinesin-1 is also involved in the lysosomal degradation.

Fig. 3 shows that there are two groups of proteins exhibiting different responses to RBL-mediated HMWS formation. One group of proteins, like c-MYC, p53, KIF5B and α-Tubulin, is sensitive to RBL. Within this group, c-MYC and p53 are nuclear transcription factors, while KIF5B and α-Tubulin are mainly cytoplasmic proteins. Both c-MYC as shown in this report and p53 are degraded in the cytoplasm [38,39]. Another group of proteins, p38MAPK, NF-κB p65, β-Actin and c-Fos, is not sensitive to RBL. Within this group, in unstimulated cells, p38MAPK and NF-κB p65 localize in the cytoplasm, while c-Fos localizes in the nucleus and β-Actin in both compartments. There is no obvious correlation between the subcellular location of a protein and RBL-mediated HMWS formation. The proteins in the latter group may or may not be degraded via the KIF5B-dependent mechanism, although their degradation rates are slow.

The results here show that KIF5B and KCL1 interact with c-MYC. Interestingly, KLC1 interacts with the scaffolding protein JLP [43], which has been shown to associate with c-MYC [14]. Therefore it is possible that JLP serves as an adapter to bring Kinesin-1 and c-MYC together. This is consistent with the findings that Kinesin uses JLP as an adapter protein to transport its cargo (endosomal vehicles) for microtubule-based endosome-to-trans-Golgi network traffic [44].

c-MYC and Kinesin-1 are related to cancer formation. Although the role of c-MYC in cancer is well established [3], the role that Kinesin-1 plays in tumor formation is not well characterized. Kinesin-1 mRNA and protein levels are elevated in several tumor types and cancer cell lines [8]. Furthermore, ablation of KIF5B shows various degrees of cytotoxicity toward cancer cells [45]. While it is advantageous for cancer cells to maintain high levels of c-MYC for cancer phenotypes [1,2], it is not known why cancer cells require Kinesin-1, if Kinesin-1 transports c-MYC to proteasomes for elimination. It is possible that Kinesin-1 is important to eliminate c-MYC 'waste'. High levels of c-MYC in cancer cells lead to the production of high levels of c-MYC 'waste' to be degraded. If the ubiquitinated c-MYC 'waste' is not cleared fast enough, it will form aggregates [46,47]. The effects may be similar to the aggregation of c-MYC in the cytoplasm induced by MG132 or RBL (Figs. 2 and 7). It is known that protein aggregates are toxic to the cells [48]. As a result, cancer cells have a higher dependency on Kinesin-1 to eliminate the c-MYC 'waste' to avoid its aggregation and the associated cytotoxicity. Furthermore, when the degradation of c-MYC is inhibited, c-MYC is accumulated in the cells, leading to the inhibition of its transformation activities (Fig. 9). Therefore, cancer cells also depend on Kinesin-1 to maintain the transformation activities of c-MYC. The findings show that Kinesin-1 is essential for proper c-MYC degradation and its

transformation activities. The dependence of cancer cells on Kinesin-1 makes Kinesin-1 an attractive therapeutic target for treatments.

In addition to its involvement in cancer formation, Kinesin-1 may have a role in neurodegenerative diseases. Kinesin-1 has been shown to transport proteins such as Tau and α-Synuclein that are implicated in the pathology of neurodegenerative diseases [49]. Both proteins form aggregates in neuronal cells. It will be interesting to determine whether Kinesin-1 also transports them to proteasomes for degradation and whether Kinesin-1 plays a role in aggregate formation of Tau and α-Synuclein proteins in the brain.

Taken together, this report links the intracellular motor Kinesin-1, c-MYC and proteasomal degradation. Kinesin-1 serves as a regulator regulator/molecular motor in the transport of c-MYC to proteasomes for degradation. Blocking of Kinesin-1 function will lead to hyper-ubiquitination and aggregation of c-MYC in the cytoplasm resulting in inhibition of transformation activities of c-MYC. Therefore, Kinesin-1 adds another layer of post-translational control of c-MYC and may provide an avenue for therapeutic intervention for c-MYC-mediated cancers.

Acknowledgements

I thank Christine Blattner, Anthony Brown, David Fedida and Manuel S. Rodriguez for the gifts of expression plasmids; E. Premkumar Reddy, Stephen C. Cosenza, Yen K. Liu, Stacey J. Baker, Richard V. Mettus, Poornima Ramkumar, Sau Ying Yip and Sol D. Gloria for their support and critical reading of the manuscript.

Appendix A. Supplementary data

Supplementary data to this article can be found online at http://dx.doi.org/10.1016/j.bbamcr.2014.05.001.

References

[1] S. Adhikary, M. Eilers, Transcriptional regulation and transformation by Myc proteins, Nat. Rev. Mol. Cell Biol. 6 (2005) 635–645.
[2] A. Albihn, J.I. Johnsen, M.A. Henriksson, MYC in oncogenesis and as a target for cancer therapies, Adv. Cancer Res. 107 (2010) 163–224.
[3] N. Meyer, L.Z. Penn, Reflecting on 25 years with MYC, Nat. Rev. Cancer 8 (2008) 976–990.
[4] J. Muller, M. Eilers, Ubiquitination of Myc: proteasomal degradation and beyond, Ernst Schering Found. Symp. Proc. (2008) 99–113.
[5] S.E. Salghetti, S.Y. Kim, W.P. Tansey, Destruction of Myc by ubiquitin-mediated proteolysis: cancer-associated and transforming mutations stabilize Myc, EMBO J. 18 (1999) 717–726.
[6] R.C. Sears, The life cycle of C-myc: from synthesis to degradation, Cell Cycle 3 (2004) 1133–1137.
[7] N. Hirokawa, S. Niwa, Y. Tanaka, Molecular motors in neurons: transport mechanisms and roles in brain function, development, and disease, Neuron 68 (2010) 610–638.
[8] Y. Yu, Y.M. Feng, The role of kinesin family proteins in tumorigenesis and progression: potential biomarkers and molecular targets for cancer therapy, Cancer 116 (2010) 5150–5160.
[9] K.J. Verhey, J.W. Hammond, Traffic control: regulation of kinesin motors, Nat. Rev. Mol. Cell Biol. 10 (2009) 765–777.
[10] N. Hirokawa, Y. Noda, Y. Tanaka, S. Niwa, Kinesin superfamily motor proteins and intracellular transport, Nat. Rev. Mol. Cell Biol. 10 (2009) 682–696.
[11] V. Gupta, K.J. Palmer, P. Spence, A. Hudson, D.J. Stephens, Kinesin-1 (uKHC/KIF5B) is required for bidirectional motility of ER exit sites and efficient ER-to-Golgi transport, Traffic 9 (2008) 1850–1866.
[12] D. Wiederschain, S. Wee, L. Chen, A. Loo, G. Yang, A. Huang, Y. Chen, G. Caponigro, Y. M. Yao, C. Lengauer, W.R. Sellers, J.D. Benson, Single-vector inducible lentiviral RNAi system for oncology target validation, Cell Cycle 8 (2009) 498–504.
[13] E.M. Blackwood, B. Luscher, R.N. Eisenman, Myc and Max associate in vivo, Genes Dev. 6 (1992) 71–80.
[14] C.M. Lee, D. Onesime, C.D. Reddy, N. Dhanasekaran, E.P. Reddy, JLP: a scaffolding protein that tethers JNK/p38MAPK signaling modules and transcription factors, Proc. Natl. Acad. Sci. U. S. A. 99 (2002) 14189–14194.
[15] S.C. Hopkins, R.D. Vale, I.D. Kuntz, Inhibitors of kinesin activity from structure-based computer screening, Biochemistry 39 (2000) 2805–2814.
[16] G. Lalli, S. Gschmeissner, G. Schiavo, Myosin Va and microtubule-based motors are required for fast axonal retrograde transport of tetanus toxin in motor neurons, J. Cell Sci. 116 (2003) 4639–4650.
[17] N. Hirokawa, R. Takemura, Molecular motors in neuronal development, intracellular transport and diseases, Curr. Opin. Neurobiol. 14 (2004) 564–573.
[18] A. Uchida, N.H. Alami, A. Brown, Tight functional coupling of kinesin-1A and dynein motors in the bidirectional transport of neurofilaments, Mol. Biol. Cell 20 (2009) 4997–5006.
[19] A.D. Zadeh, Y. Cheng, H. Xu, N. Wong, Z. Wang, C. Goonasekara, D.F. Steele, D. Fedida, Kif5b is an essential forward trafficking motor for the Kv1.5 cardiac potassium channel, J. Physiol. 587 (2009) 4565–4574.
[20] R. Hjerpe, M.S. Rodriguez, Efficient approaches for characterizing ubiquitinated proteins, Biochem. Soc. Trans. 36 (2008) 823–827.
[21] S.Y. Kim, A. Herbst, K.A. Tworkowski, S.E. Salghetti, W.P. Tansey, Skp2 regulates Myc protein stability and activity, Mol. Cell 11 (2003) 1177–1188.
[22] I. Paul, S.F. Ahmed, A. Bhowmik, S. Deb, M.K. Ghosh, The ubiquitin ligase CHIP regulates c-Myc stability and transcriptional activity, Oncogene 32 (2013) 1284–1295.
[23] M. Yada, S. Hatakeyama, T. Kamura, M. Nishiyama, R. Tsunematsu, H. Imaki, N. Ishida, F. Okumura, K. Nakayama, K.I. Nakayama, Phosphorylation-dependent degradation of c-Myc is mediated by the F-box protein Fbw7, EMBO J. 23 (2004) 2116–2125.
[24] M. Welcker, A. Orian, J.E. Grim, R.N. Eisenman, B.E. Clurman, A nucleolar isoform of the Fbw7 ubiquitin ligase regulates c-Myc and cell size, Curr. Biol. 14 (2004) 1852–1857.
[25] L.A. Huber, S. Pimplikar, R.G. Parton, H. Virta, M. Zerial, K. Simons, Rab8, a small Gtpase involved in vesicular traffic between the Tgn and the basolateral plasma-membrane, J. Cell Biol. 123 (1993) 35–45.
[26] M. Fukuda, S. Asano, T. Nakamura, M. Adachi, M. Yoshida, M. Yanagida, E. Nishida, CRM1 is responsible for intracellular transport mediated by the nuclear export signal, Nature 390 (1997) 308–311.
[27] M.A. Welte, Bidirectional transport along microtubules, Curr. Biol. 14 (2004) R525–R537.
[28] J. Luders, T. Stearns, Microtubule-organizing centres: a re-evaluation, Nat. Rev. Mol. Cell Biol. 8 (2007) 161–167.
[29] M. Dean, R.A. Levine, W. Ran, M.S. Kindy, G.E. Sonenshein, J. Campisi, Regulation of c-myc transcription and mRNA abundance by serum growth factors and cell contact, J. Biol. Chem. 261 (1986) 9161–9166.
[30] V. Daire, J. Giustiniani, I. Leroy-Gori, M. Quesnoit, S. Drevensek, A. Dimitrov, F. Perez, C. Pous, Kinesin-1 regulates microtubule dynamics via a c-Jun N-terminal kinase-dependent mechanism, J. Biol. Chem. 284 (2009) 31992–32001.
[31] D.H. Lee, A.L. Goldberg, Proteasome inhibitors cause induction of heat shock proteins and trehalose, which together confer thermotolerance in Saccharomyces cerevisiae, Mol. Cell. Biol. 18 (1998) 30–38.
[32] N. Hirokawa, Y. Noda, Intracellular transport and kinesin superfamily proteins, KIFs: structure, function, and dynamics, Physiol. Rev. 88 (2008) 1089–1118.
[33] R. Kulikov, J. Letienne, M. Kaur, S.R. Grossman, J. Arts, C. Blattner, Mdm2 facilitates the association of p53 with the proteasome, Proc. Natl. Acad. Sci. U. S. A. 107 (2010) 10038–10043.
[34] J. Barrett, M.J. Birrer, G.J. Kato, H. Dosaka-Akita, C.V. Dang, Activation domains of L-Myc and c-Myc determine their transforming potencies in rat embryo cells, Mol. Cell. Biol. 12 (1992) 3130–3137.
[35] K.J. Verhey, T.A. Rapoport, Kinesin carries the signal, Trends Biochem. Sci. 26 (2001) 545–550.
[36] C. Wojcik, G.N. DeMartino, Intracellular localization of proteasomes, Int. J. Biochem. Cell Biol. 35 (2003) 579–589.
[37] A.J. Rivett, Intracellular distribution of proteasomes, Curr. Opin. Immunol. 10 (1998) 110–114.
[38] Y. Zhang, Y. Xiong, Control of p53 ubiquitination and nuclear export by MDM2 and ARF, Cell Growth Differ. 12 (2001) 175–186.
[39] D. Michael, M. Oren, The p53-Mdm2 module and the ubiquitin system, Semin. Cancer Biol. 13 (2003) 49–58.
[40] H.C. Tai, E.M. Schuman, Ubiquitin, the proteasome and protein degradation in neuronal function and dysfunction, Nat. Rev. Neurosci. 9 (2008) 826–838.
[41] A. Ciechanover, Intracellular protein degradation: from a vague idea thru the lysosome and the ubiquitin–proteasome system and onto human diseases and drug targeting, Biochim. Biophys. Acta 1824 (2012) 3–13.
[42] A. Williams, L. Jahreiss, S. Sarkar, S. Saiki, F.M. Menzies, B. Ravikumar, D.C. Rubinsztein, Aggregate-prone proteins are cleared from the cytosol by autophagy: therapeutic implications, Curr. Top. Dev. Biol. 76 (2006) 89–101.
[43] Q. Nguyen, C.M. Lee, A. Le, E.P. Reddy, JLP associates with kinesin light chain 1 through a novel leucine zipper-like domain, J. Biol. Chem. 280 (2005) 30185–30191.
[44] O.C. Ikonomov, J. Fligger, D. Sbrissa, R. Dondapati, K. Mlak, R. Deeb, A. Shisheva, Kinesin adapter JLP links PIKfyve to microtubule-based endosome-to-trans-Golgi network traffic of furin, J. Biol. Chem. 284 (2009) 3750–3761.
[45] C.M. Cardoso, L. Groth-Pedersen, M. Hoyer-Hansen, T. Kirkegaard, E. Corcelle, J.S. Andersen, M. Jaattela, J. Nylandsted, Depletion of kinesin 5B affects lysosomal distribution and stability and induces peri-nuclear accumulation of autophagosomes in cancer cells, PLoS ONE 4 (2009) e4424.
[46] Z. Li, L. Arnaud, P. Rockwell, M.E. Figueiredo-Pereira, A single amino acid substitution in a proteasome subunit triggers aggregation of ubiquitinated proteins in stressed neuronal cells, J. Neurochem. 90 (2004) 19–28.
[47] J. Hai, Q. Lin, S.H. Su, L. Zhang, J.F. Wan, Y. Lu, Chronic cerebral hypoperfusion in rats causes proteasome dysfunction and aggregation of ubiquitinated proteins, Brain Res. 1374 (2011) 73–81.
[48] M. Stefani, Protein aggregation diseases: toxicity of soluble prefibrillar aggregates and their clinical significance, Methods Mol. Biol. 648 (2010) 25–41.
[49] M.A. Utton, W.J. Noble, J.E. Hill, B.H. Anderton, D.P. Hanger, Molecular motors implicated in the axonal transport of tau and alpha-synuclein, J. Cell Sci. 118 (2005) 4645–4654